Supporting Information

Luksys et al. 10.1073/pnas.1500860112

SI Materials and Methods

Array-Based SNP Genotyping. Blood was drawn by using 2 × 9 mL EDTA tubes (Sarstedt). Saliva was collected with the Oragene DNA sample collection kit (DNA Genotek Inc.). DNA isolation was done according to standard protocols. Samples were processed as described in the Genome-Wide Human SNP Nsp/Sty 6.0 User Guide (Affymetrix). Briefly, the genomic DNA concentration was determined by using a Nano-Drop ND-1000 and was adjusted to 50 ng/μL in water. DNA (250 ng) was digested in parallel with 10 units of StyI and NspI restriction enzymes (New England Biolabs) for 2 h at 37 °C. Enzyme-specific adaptor oligonucleotides then were ligated onto the digested ends with T4 DNA Ligase for 3 h at 16 °C. After adjustment to 100 μL with water, 10 μL of the diluted ligation reactions were subjected to PCR. Three PCR reactions of 100 μL were performed for StyI-digested products, and four PCR reactions were performed for NspI-digested products. PCR was performed with Titanium Taq DNA Polymerase (Clontech) in the presence of 4.5 μM PCR primer 002 (Affymetrix), 350 μM each dNTP (Clontech), 1 M G-C Melt (Clontech), and 1× Titanium Taq PCR Buffer (Clontech). Cycling parameters were as follows: initial denaturation at 94 °C for 3 min, amplification at 94 °C for 30 s, 60 °C for 45 s, and extension at 68 °C for 15 s, repeated a total of 30 times, with a final extension at 68 °C for 7 min. Reactions then were verified to migrate at an average size of 200–1,100 bp using 2% TBE gel electrophoresis. PCR products were combined and purified with the Filter Bottom Plate (Seahorse Bioscience) using Agencourt Magnetic Beads (Beckman Coulter). Purified PCR products were quantified on a Zenyth 200rt microplate reader (Anthos Labtec). On average, 4–5 μg/μL were obtained for each sample. From this stage on, the SNP Nsp/Sty 5.0/6.0 Assay Kit (Affymetrix) was used. Around 250 μg of purified PCR products were fragmented using 0.5 units of DNaseI at 37 °C for 35 min. Fragmentation of the products to an average size of less than 180 bp was verified using 4% Tris-borate-EDTA gel electrophoresis. Following fragmentation, the DNA was end-labeled with 105 units of terminal deoxynucleotidyl transferase at 37 °C for 4 h. The labeled DNA then was hybridized onto a Genome-Wide Human SNP 6.0 Array at 50 °C for 18 h at 60 rpm (Affymetrix GeneChip Hybridization Oven 645, Rotisserie 00-0331). The hybridized array was washed, stained, and scanned according to the manufacturer's (Affymetrix) instructions using Affymetrix GeneChip Command Console (AGCC version 3.0.1.1214). Generation of SNP calls and Array QC were performed using the command line programs of the Affymetrix Power Tools package (version: apt-1.14.2). According to the manufacturer's recommendation, Contrast QC was chosen as the QC metric, using the default value of greater or equal than 0.4. The mean call rate for all samples averaged >98.5%. All samples passing QC criteria were subsequently genotyped using the Birdseed (v2) algorithm.

fMRI Data Acquisition and Preprocessing. Measurements were performed on a Siemens MAGNETOM Verio 3-T whole-body MR unit equipped with a 12-channel head coil. Functional time series were acquired with a single-shot echo-planar sequence using parallel imaging (GRAPPA). We used the following acquisition parameters: echo time (TE) = 35 ms, field of view (FOV) = 22 cm; acquisition matrix = 80 × 80; interpolated to 128 × 128; voxel size: 2.75 × 2.75 × 4 mm^3; GRAPPA acceleration factor R = 2.0. Using a midsagittal scout image, 32 contiguous axial slices placed along the anterior–posterior commissure (AC–PC) plane covering the entire brain with a TR = 3,000 ms (α = 82°) were acquired using an ascending interleaved sequence. A high-resolution T1-weighted anatomical image was acquired using a magnetization prepared gradient echo sequence (MPRAGE, TR = 2,000 ms; TE = 3.37 ms; TI = 1,000 ms; flip angle = 8°; 176 slices; FOV= 256 mm).

Preprocessing and data analysis were performed using SPM8 (Statistical Parametric Mapping, Wellcome Trust Centre for Neuroimaging; www.fil.ion.ucl.ac.uk/spm/) implemented in MATLAB R2011b (MathWorks Inc.). Volumes were slice-time corrected to the first slice and realigned using the "register to mean" option. A mean image was generated from the realigned series and coregistered to the structural image, ensuring that functional and structural images were spatially aligned.

The functional images and the structural images were spatially normalized by applying DARTEL, which leads to an improved registration between subjects. Normalization incorporated the following steps: (*i*) Structural images of each subject were segmented using the "New Segment" procedure in SPM8. (*ii*). The resulting gray- and white-matter images were used to derive a study-specific group template. The template was computed from a large population of 1,000 subjects that included the 795 subjects from this study. (*iii*) An affine transformation was applied to map the group template to MNI space. (*iv*) Subject-to-template and template-to-MNI transformations were combined to map the functional images to MNI space. The functional images were smoothed with an isotropic 8-mm FWHM Gaussian filter.

For each subject, analyses were conducted in the framework of the general linear model (GLM). Regressors modeling the onsets and duration of stimulus events were convolved with a canonical hemodynamic response function. More precisely, the model comprised regressors for button presses modeled as stick/delta functions, picture presentations modeled with an epoch/boxcar function (duration: encoding: 2.5 s; retrieval: 1 s), and rating scales modeled with an epoch/boxcar function of variable duration (depending on when the subsequent button press occurred). Serial correlations were removed using a first-order autoregressive model, and a high-pass filter (128 s) was applied to remove low-frequency noise. Six movement parameters were also entered as nuisance covariates. Pictures accounting for possible primacy and recency effects were excluded from statistical analysis.

fMRI Group Statistics. EPI sequences suffer from signal loss in the presence of magnetic field inhomogeneities that can occur close to air–tissue boundaries. The normalization procedure applied in DARTEL accurately transforms both voxels with signal and voxels with signal loss to MNI space. In SPM8, signal loss at an MNI coordinate in a functional image of only one subject leads to the exclusion of the voxel at this coordinate from the group-level analysis. Therefore, the probability of a voxel being excluded increases with sample size. GLM Flex circumvents this problem by allowing a variable number of subjects at each voxel (Martinos Center, Massachusetts General Hospital; mrtools.mgh.harvard.edu). The minimum number of subjects per voxel was set to 400.

German AgeCoDe Sample: Selection of Participants. Participants were recruited between January 2003 and November 2004 in six German study centers (Bonn, Duesseldorf, Hamburg, Leipzig, Mannheim, and Munich) via general practitioners (GPs) connected with the respective study sites. Inclusion criteria were age of 75 y or older, absence of dementia (according to the GP's judgment), and at least one contact with the GP within

the last 12 mo. Exclusion criteria were GP consultations by home visits only, residence in a nursing home, presence of a severe illness with an anticipated fatal outcome within 3 mo, insufficient German language abilities, deafness or blindness, lack of ability to provide an informed consent, and status as being only an occasional patient of the participating GP. A total of 3,327 subjects were contacted successfully and assessed with structured clinical interviews at their homes. A total of 110 individuals were excluded after the first interview because of the presence of dementia or an actual age below 75 y (falsely classified as age 75 y or older in the sample-selection process). For the present analyses, data from baseline and three follow-up measurements at 18-mo intervals were available. In a primary care-based sample of older individuals, conditions can be present that affect cognition and the reliability of neuropsychological tests. To generate a sample of healthy elderly individuals, we further used the following selection criteria at baseline: age between 75 and 90 y, German as native language, at least a school-leaving certificate, absence of severe hearing or vision impairments, absence of insufficient test motivation as judged by the interviewer, absence of disturbing factors during neuropsychological testing, and absence of all the following comorbid conditions: Parkinson's disease, epilepsy, alcohol abuse, stroke, multiple sclerosis, evidence of depression (a score of 6 or higher on the Geriatric Depression Scale), traumatic brain injury with unconsciousness of more than 30 min, visible neurological malfunctions, and dementia according to *Diagnostic and Statistical Manual of Mental Disorders-IV* criteria. In addition, we excluded subjects who converted to dementia before the third follow-up (i.e., within 4.5 y after baseline) or for whom neuropsychological test data were not available at baseline and all follow-up visits.

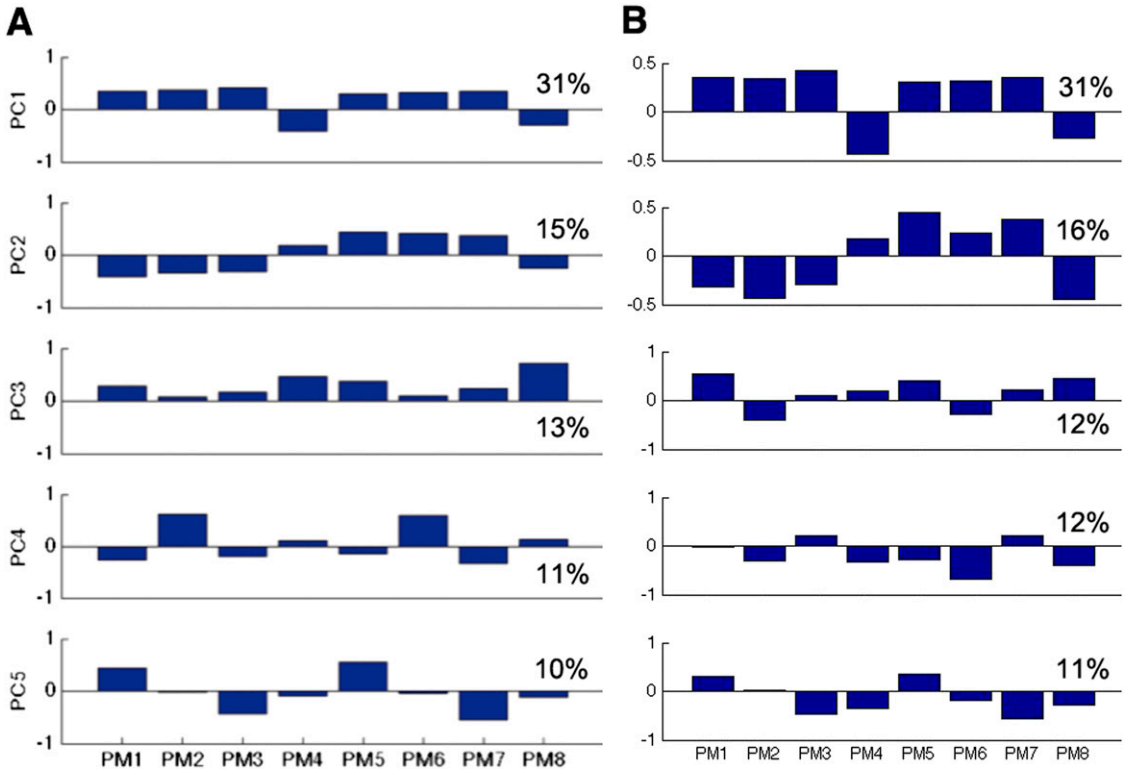

Fig. S1. PCA of eight performance measures (PM1–PM8, described in Table 2) in the discovery sample (*A*) (modified from ref. 21) and the replication sample (*B*). Percentages denote variance explained by each component. The first five principal components (PC_{1-5}) explain more than 80% of the variance in the data; their loadings suggest that the first component (PC_1) can be approximately related to general learning ability and the second one (PC_2) to delayed memory recall (compared with immediate recall). The latter three components could be interpreted only in the discovery sample: PC_3 related approximately to errors, PC_4 to the recall of negative words, and PC_5 to the recall of positive minus neutral words.

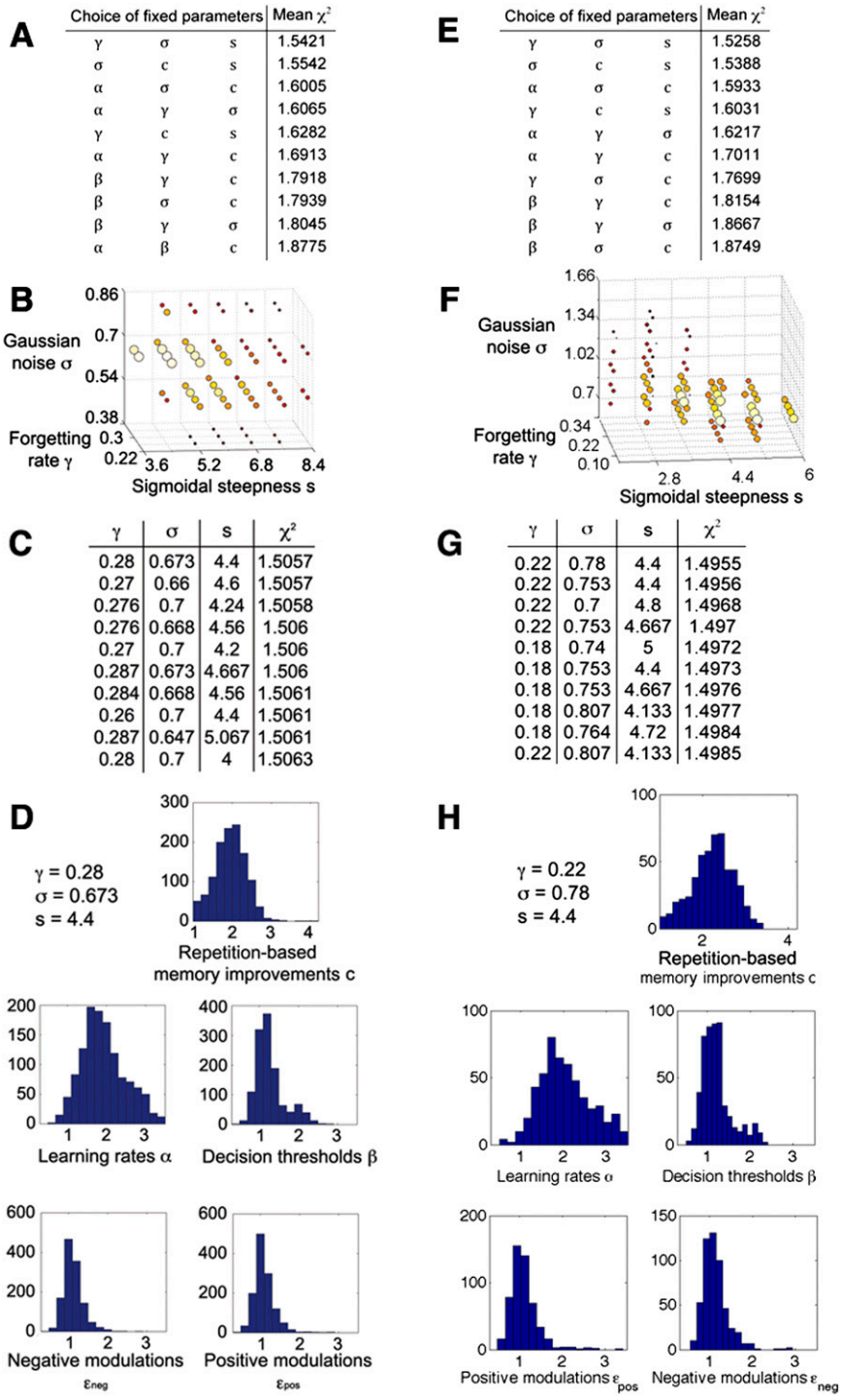

Fig. S2. Parameter estimation results for the discovery sample (*A–D*) (modified from ref. 21) and the replication sample (*E–H*). (*A* and *E*) Stage 1: Based on a moderately accurate estimation of model parameters, two selections of fixed parameters (γ, σ, *s* and σ, *c*, *s*) are chosen for hill climbing. The best 10 of all 56 possible three-of-eight combinations are shown. (*B* and *F*) Stage 2: The hill-climbing results of estimating three fixed parameters for the best model (with Gaussian noise σ, sigmoidal steepness *s*, and forgetting rate γ fixed) are shown, with bigger circles and lighter colors indicating better goodness-of-fit; the 10 best hill-climbing points (biggest light yellow circles) were selected for evaluating averages of all their possible combinations. (*C* and *G*) Stage 3: The 10 combinations with the best goodness-of-fit (χ^2) are displayed. Overall, 267 of 1,023 combinations had better χ^2 than the best hill-climbing point ($\chi^2 = 1.522$) for the discovery sample, as did 77 of 1,023 combinations for the replication sample ($\chi^2 = 1.507$), suggesting that averaging parameters helps overcome gaps in step size and leads to refined parameter values. (*D* and *H*) Histograms of the best-fitting individual parameters show distributions with the following means: $c = 1.95$, $\alpha = 1.93$, $\beta = 1.27$, $\varepsilon_{neg} = 1.12$, $\varepsilon_{pos} = 1.09$ for the discovery sample and $c = 2.23$, $\alpha = 2.04$, $\beta = 1.22$, $\varepsilon_{neg} = 1.13$, $\varepsilon_{pos} = 1.11$ for the replication sample.

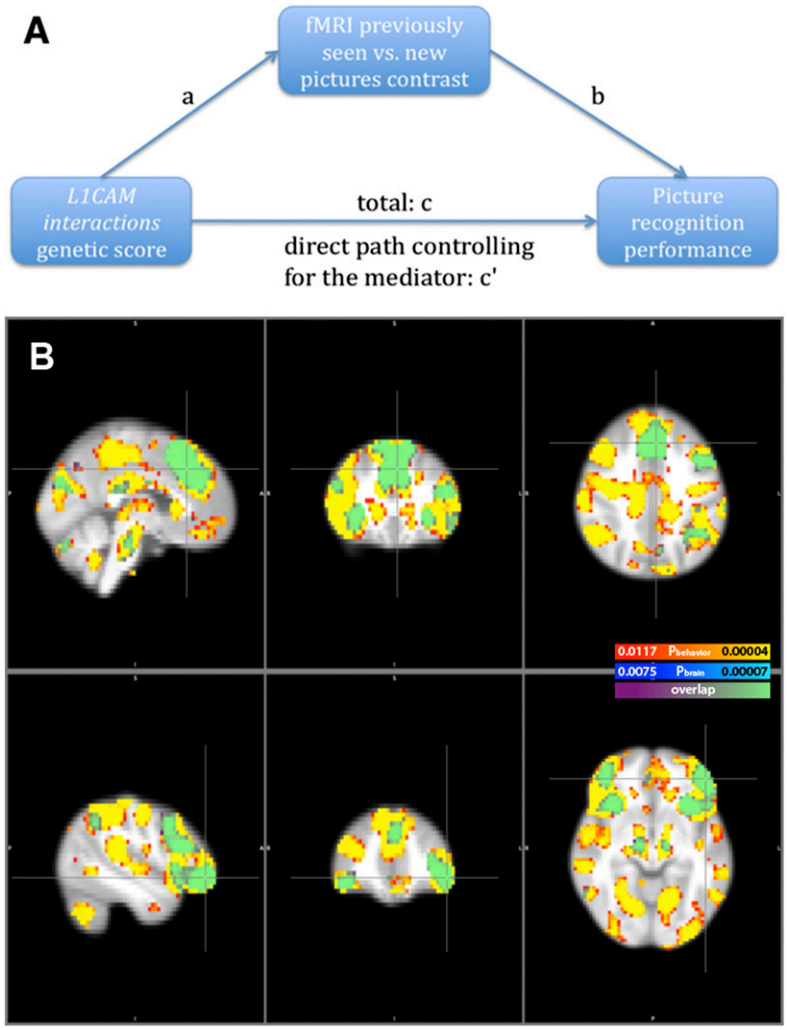

Fig. S3. Scheme and results of the mediation analysis. (*A*) The overall predictor–outcome relationship is denoted as "c," and the direct effect controlling for the mediator is denoted as "c′." The a × b effect tests the significance of mediation (c–c′). For more details see *Materials and Methods*. (*B*) Mediation results at (−3, 28, 40) and (−47, 44, −8), depicting voxels for which the contrast in brain activation related to the previously seen vs. new pictures was considered a significant mediator of the relationship between the genetic score and recognition performance (blue scale), at a significance threshold of *P*(FDR) = 0.0075. The value of this threshold for whole-brain correction might be unusually high because of correlations between the genetic score and the behavioral phenotype. As a control, random shuffling of fMRI images between subjects was performed 10 times, always leading to no voxels surviving the FDR significance threshold. We also found that behavioral phenotype was a significant mediator of the relationship between the genetic score and differences in brain activity. Results are shown based on the red-to-yellow scale, superimposed on the original ones, at a significance threshold of *P*(FDR) = 0.0117. Effect sizes with neuroimaging and behavioral phenotypes as mediators were comparable in the four clusters associated with the genetic score. For the coronal and horizontal sections left in the picture refer to the right side of the brain and vice versa.

Table S1. Correlations of estimated model parameters with related behavioral measures of verbal task performance in the discovery sample and picture task performance in the replication (words/pictures) sample

Model parameter	Relevant phenotype in the verbal task	Correlation, Spearman's ρ	Relevant free recall phenotype in the picture task	Correlation, Spearman's ρ
Learning rate α	Percentage of correctly remembered words in the immediate recall	0.722	Percentage of correctly remembered pictures	0.152
Decision threshold β	Number of mistakes in the delayed recall	−0.825	Number of mistakes in the picture recall	−0.204
Repetition-based memory improvement *c*	Percentage of correctly remembered words in the delayed recall	0.607	Percentage of correctly remembered pictures	0.098
Modulation by positive emotional arousal ε_{pos}	Percentage of correctly remembered positive minus neutral words in the delayed recall	0.737	Percentage of correctly remembered positive minus neutral pictures	0.133
Modulation by negative emotional arousal ε_{neg}	Percentage of correctly remembered negative minus neutral words in the delayed recall	0.708	Percentage of correctly remembered negative minus neutral pictures	0.074

Correlations with verbal task performance are quite high because computational modeling was performed for the verbal task. Correlations with picture task performance suggest that the percentage of correctly remembered pictures in the free recall is related more to the learning rate α than to the repetition-based memory improvement *c* and hence is used for the replication of gene sets associated with α. All correlations are statistically significant.

Table S2. Composition of the L1CAM interactions genetic score: SNP IDs, tagged genes, statistics of association with picture recognition in the pictures/fMRI sample, reference allele with direction of association with picture recognition memory, major allele

SNP rsID	Gene symbol	Association *P* value	Reference allele	Direction of association	Major allele
rs9459771	*RPS6KA2*	0.0011	T	+	C
rs11715984	*DLG1*	0.0017	G	+	A
rs13258436	*KCNQ3*	0.0020	T	+	C
rs197721	*ITGA9*	0.0049	T	+	G
rs7153298	*RPS6KA5*	0.0071	T	−	T
rs17210194	*CNTN6*	0.0110	G	−	G
rs3506	*AP2B1*	0.0113	T	+	T
rs17547685	*SH3GL2*	0.0130	T	−	T
rs17333297	*NRCAM*	0.0149	G	−	A
rs6983315	*FGFR1*	0.0185	G	+	G
rs11009157	*ITGB1*	0.0195	G	−	G
rs4948381	*ANK3*	0.0235	G	+	A
rs442103	*DPYSL2*	0.0247	G	−	G
rs10504047	*ANK1*	0.0254	G	−	C
rs1478438	*ITGA1*	0.0267	T	−	T
rs7781264	*EGFR*	0.0281	T	+	C
rs645078	*RPS6KA4*	0.0311	C	−	A
rs11647503	*CSNK2A2*	0.0318	T	+	C
rs949215	*LAMA1*	0.0318	C	−	C
rs6580842	*SCN8A*	0.0335	G	+	A
rs883501	*NRP2*	0.0335	T	+	A
rs1421933	*ITGA2*	0.0352	G	−	G
rs17115275	*NCAM1*	0.0352	G	−	A
rs7643664	*ALCAM*	0.0360	C	+	C
rs16943748	*CLTC*	0.0369	G	+	G
rs6793943	*SCN5A*	0.0407	T	+	C
rs11240351	*CNTN2*	0.0407	T	+	T
rs1331325	*NRP1*	0.0407	T	−	C

Table S3. Association between differences in brain activity during picture recognition and the L1CAM interactions genetic score that uses the two most significant SNPs per gene

Regional correspondence of the maximum	Left/right	No. of voxels	Peak MNI coordinates			Peak statistics	
			X	Y	Z	T	$P_{nominal}$
Superior frontal cortex (80%)	Left	76	−3	30	40	−5.77	1.1×10^{-8}
Pars orbitalis cortex (56%), pars triangularis cortex (22%), rostral middle frontal cortex (4%)	Left	23	−47	41	−12	−5.42	8.0×10^{-8}
Pars orbitalis cortex (35%), rostral middle frontal cortex (1%)	Right	23	41	44	−12	−5.37	1.0×10^{-7}
Lateral orbitofrontal cortex (20%), insula (23%)	Right	21	30	22	0	−5.32	1.3×10^{-7}
Superior frontal cortex (84%)	Right	3	11	28	60	−5.02	6.2×10^{-7}

The fMRI contrast between previously seen vs. new pictures was used. Only clusters with at least three voxels surviving whole-brain FWE correction are shown (P whole-brain FWE-corrected < 0.05; $|T| > 4.77$; $n = 795$). Region names are in accordance with the FreeSurfer nomenclature (71); probabilities are in accordance with the in-house atlas.

Table S4. Association between differences in brain activity during picture recognition (fMRI contrast of previously seen vs. new pictures) and the percentage of correctly recollected pictures

Regional correspondence of the maximum	Left/right	MNI coordinates at the maximum			T value
		X	Y	Z	
Superior frontal cortex (79%), caudal anterior cingulate cortex (2%)	Left	−3	28	40	−12.13
Pars orbitalis cortex (34%), pars triangularis cortex (28%), rostral middle frontal cortex (16%)	Left	−47	44	−8	−9.11
Lateral orbitofrontal cortex (20%), insula (23%)	Right	30	22	0	−9.08
Lateral orbitofrontal cortex (73%), insula (8%)	Left	−28	22	−4	−9.65

Test statistics are shown at the maxima of clusters associated with the L1CAM interactions genetic score (Table 6). They indicate that differences in brain activity at these clusters are also associated with picture recognition performance in the same direction as the L1CAM interactions genetic score. Region names are in accordance with the FreeSurfer nomenclature (71); probabilities are in accordance with the in-house atlas.

Table S5. Tagging SNPs of the amine compound SLC transporters gene set

Gene symbol	Tagging SNP in the discovery sample	Tagging SNP in the replication sample and its LD with the discovery SNP		Tagging SNP in the pictures/fMRI sample and its LD with the discovery SNP		Tagging SNP in the words/pictures sample and its LD with the discovery SNP		Tagging SNP in the AgeCoDe sample and its LD with the discovery SNP	
SLC6A11	rs6442209	rs746278	0.0054	rs9868537	0.1251	rs1601370	0.0192	rs966030	0.0055
SLC14A2	rs7232775	rs7226686	0.0068	rs7232775	1	rs17670646	0.0845	rs4890292	0.0256
SLC6A20	rs17279437	rs7653640	0.0077	rs2251109	0.097	rs17213127	0.0058	rs11718841	0.017
SLC6A2	rs734980	rs1861646	0.004	rs36016	0.0106	rs879522	0.0118	rs10521329	0.0006
SLC44A3	rs7550014	rs11165265	0.0191	rs3849308	0.0297	rs859064	0.3058	rs7550014	1
SLC6A6	rs2164576	rs17308574	0.016	rs3773167	0.0162	rs4685160	0.1064	rs6774615	0.0685
SLC6A7	rs3776087	rs9885318	0.2705	rs3776087	1	rs4601032	0.0252	rs3776087	1
SLC6A18	rs13361701	rs6554678	0.0822	rs13361701	1	rs7704728	0.0489	rs6554677	0.1335
SLC18A2	rs363334	rs363224	0.0007	rs363223	0.0006	rs363278	0.0023	rs363271	0

For each gene listed in Table 7, the corresponding tagging (i.e., the most significant) SNP in each sample is shown together with its linkage disequilibrium (LD) r^2 value with the tagging SNP from the discovery sample. Gene descriptions, chromosome numbers, and association P values are provided in Table 7.

Table S6. Tagging SNPs of the L1CAM interactions gene set

Gene symbol	Tagging SNP in the discovery sample	Tagging SNP in the replication sample and its LD with the discovery SNP		Tagging SNP in the pictures/fMRI sample and its LD with the discovery SNP		Tagging SNP in the AgeCoDe sample and its LD with the discovery SNP	
RPS6KA2	rs2281143	rs1894660	0.0009	rs9459771	0.0005	rs9459777	0.0008
KCNQ3	rs2597348	rs2721905	0.1884	rs13258436	0.0091	rs1457784	0.0006
DPYSL2	rs7829347	rs17322275	0.0244	rs442103	0.0083	rs9314325	0.0935
ITGA9	rs399703	rs197763	0.8689	rs197721	0.057	rs6782856	0
ANK3	rs11593565	rs4948254	0.0053	rs4948381	0.001	rs12355908	0.0107
CNTN6	rs1353825	rs9880762	0.0007	rs17210194	0.0102	rs3772295	0.1717
SH3GL2	rs10491540	rs1998247	0.0414	rs17547685	0.0092	rs3808776	0.0101
SCN2A	rs353128	rs13025009	0	rs13023748	0.1728	rs10497258	0.0004
FGFR1	rs11777067	rs2288696	0.0958	rs6983315	0.3326	rs2978073	0.003
NRCAM	rs6466228	rs425013	0.0114	rs17333297	0.0019	rs404287	0.0313
ITGA1	rs870992	rs7718758	0.0224	rs1478438	0.0518	rs2938793	0
LAMA1	rs11661841	rs10163962	0.1539	rs949215	0.0009	rs8084092	0.0085
EGFR	rs6593210	rs11238349	0.0017	rs7781264	0.0123	rs4947986	0.0606
NCAM1	rs17115275	rs884110	0.0109	rs17115275	1	rs1245135	0.0038
SPTBN1	rs6545424	rs10166797	0.0988	rs6715538	0.0069	rs17343939	0.1586
CSNK2A2	rs1393203	rs37358	0.0706	rs11647503	0.0063	rs2550362	0.0203
ANK1	rs7823955	rs11784321	0.0266	rs10504047	0.5597	rs2304872	0.0052
ITGA2	rs153141	rs1421940	0.6648	rs1421933	0.0069	rs1421933	0.0282
CNTN1	rs1119060	rs10784951	0.0219	rs12829787	0.0237	rs7970805	0.0116
NRP2	rs849581	rs849570	0.7338	rs883501	0.0027	rs3771000	0.0004
NRP1	rs2506150	rs1331312	0.0144	rs1331325	0.005	rs2243668	0.0008

For each gene listed in Table 8, the corresponding tagging (i.e., the most significant) SNP in each sample is shown together with its LD r^2 value with the tagging SNP from the discovery sample. Gene descriptions, chromosome numbers, and association *P* values are provided in Table 8.